AIAA JOURNAL
Vol. 47, No. 10, October 2009

# Aerodynamic Modification of a NACA 0012 Airfoil by Trailing-Edge Plasma Gurney Flap

P. F. Zhang,* A. B. Liu,† and J. J. Wang‡
*Beijing University of Aeronautics and Astronautics, 100191 Beijing, People's Republic of China*

DOI: 10.2514/1.43379

**The effect of a novel plasma Gurney flap on the aerodynamic characteristics of a NACA 0012 airfoil is studied by solving the Reynolds-averaged Navier–Stokes equations. The plasma actuator is simulated with a phenomenological model. The results indicate that the plasma Gurney flap can increase the lift and nose-down pitching moment of the airfoil, and the mechanism is the same as that of the conventional Gurney flap. The flowfield presents that the von Kármán vortex street disappears near the trailing edge of the airfoil with a plasma Gurney flap, which decreases the airfoil's drag and thus increases the lift-to-drag ratio before stall. By comparing the lift and nose-down pitching moment increments with the conventional Gurney flap and the jet Gurney flap, the equivalent height or jet blowing momentum coefficient of the plasma Gurney flap are estimated.**

## Introduction

THE Gurney flap is a small tab attached to the pressure surface of the airfoil at a right angle in the vicinity of the trailing edge, with a height that can vary from 1 to 5% of the airfoil chord (the detail of the configuration is shown in Fig. 1). This trailing-edge device can improve the performance of a simple airfoil to nearly the same level as a complex high-performance device. Originally, the Gurney flap was installed at the trailing edge of a rectangular racing car wing by Dan Gurney, a car driver in the 1960s and 1970s, to improve the downforce with the flap.

The Gurney flap had been used in racing for several years before its true purpose became well known. In 1978, Liebeck [1] conducted the first significant wind-tunnel experiment with Gurney flaps and introduced this concept to the aerodynamic community. The results showed a significant lift increment for the Newman airfoil with a Gurney flap compared with the baseline. In general, the drag of the airfoil increases with the addition of a Gurney flap, but the lift increment is relatively greater, resulting in an lift-to-drag ratio increment and therefore a better performance of the airfoil. Liebeck suggested that the optimal height of the Gurney flap should be on the order of 1–2% of the airfoil chord. Based on the data of different investigators, Giguère et al. [2] indicated that the proper scaling parameter should be the boundary-layer thickness of the pressure side at the trailing edge of the baseline airfoil. For optimal Gurney flap performance, it turns out to be most important that the flap should be submerged within the boundary layer.

In his wind-tunnel experiment, Liebeck [1] noted that separation bubbles appeared near the trailing edge of the airfoils with a thick trailing edge or at moderate lift coefficient. When the Gurney flap is applied, two regions of separated flow appear: a small bubble just upstream of the flap and a pair of counter-rotating vortices downstream of the flap (see Fig. 2). As a result of this downstream vortical wake, the flow over the upper surface remains attached to the airfoil's trailing edge, which eliminates the separated flow. Later dye-flow experiments in a water tunnel [3] and numerical studies [4] supported Liebeck's [1] hypothesis. Jang et al. [4] stated that the mechanism responsible for the Gurney flap effect is a violation of the Kutta condition at the trailing edge, because the flap moves the stagnation point at the trailing edge toward the pressure surface. The violation of the Kutta condition, in essence, causes a pressure difference at the trailing edge. According to Jeffrey et al. [5], it is this pressure difference that causes increased loading over the airfoil. The drag increased slightly with the introduction of a Gurney flap. The data presented by Jeffrey et al. indicated that a pair of counter-rotating vortices formed downstream of the flap. These vortices are nonstationary and equal to a von Kármán vortex street.

Because of its simple geometry, the construction of the Gurney flap is simple, the weight is low, and the implementation of the flap system can be easily accomplished. Gurney flaps have been extensively investigated and used in many applications (e.g., alleviation of airfoil static and dynamic stall [6,7], flutter control [8,9], and rotor blade load control [10]). Except for two-dimensional Gurney flaps, three-dimensional Gurney flaps were used to modify the aerodynamic performance of rectangular wing [11], delta wing [12], and other aircraft models, such as forward-swept-wing aircraft [13] and micro air vehicles [14]. More details about the Gurney flap applications and the effects of configuration parameters such as position, mounting angle, etc., can be seen in the review paper by Wang et al. [15]. In these applications, a Gurney flap was found to enhance the lift. The drag penalty varies depending on the airfoils used, the Gurney flap configurations, and the flow conditions.

As mentioned already, the simple mini Gurney flap can enhance the lift of airfoils, wings, and aircraft models, but it also introduces drag increment. Although the maximum lift-to-drag ratio can be optimized by using a small Gurney flap immerged in the boundary layer on the lower surface of the airfoil trailing edge, it is not a good solution to the drag increase of the aircraft in cruise at low angles of attack.

Meyer et al. [16] indicated that the drag increment associated with the Gurney flap may be lessened by creating discontinuities in the flap. The discontinuities serve to introduce three-dimensional flow into the wake, helping to attenuate the von Kármán vortex street that has been observed to form downstream of the flap. They used slits and holes in the Gurney flap to stabilize the wake downstream of the trailing edge of HQ17 and FX73 airfoils. The drag can be reduced by these devices compared with that of the airfoil with a standard Gurney flap, but is still larger than a clean airfoil.

From previous investigations, it can be concluded that it is impossible for a static Gurney flap to keep the same drag value as a clean airfoil. To apply a Gurney flap to the engineering, the only way is to design an active Gurney flap, which can be retracted during cruise to decrease drag. But it is quite difficult to design such a mechanical structure near the trailing edge, which is too slim to contain the moving parts. The strength of the structure will also be

Received 22 January 2009; revision received 30 June 2009; accepted for publication 30 June 2009. 

*Associate Professor, Institute of Fluid Mechanics; pfzhang@buaa.edu.cn.
†Graduate Student, Institute of Fluid Mechanics; aibingliu@gmail.com.
‡Professor, Institute of Fluid Mechanics; jjwang@buaa.edu.cn. Member AIAA.

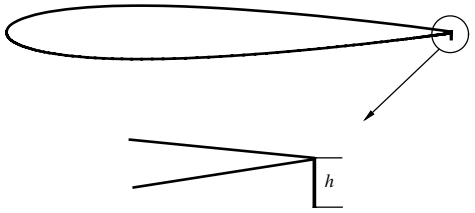


**Fig. 1 Typical configuration of a Gurney flap on a NACA 0012 airfoil.**

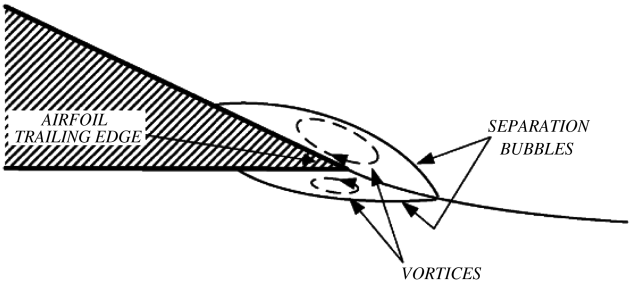


a)

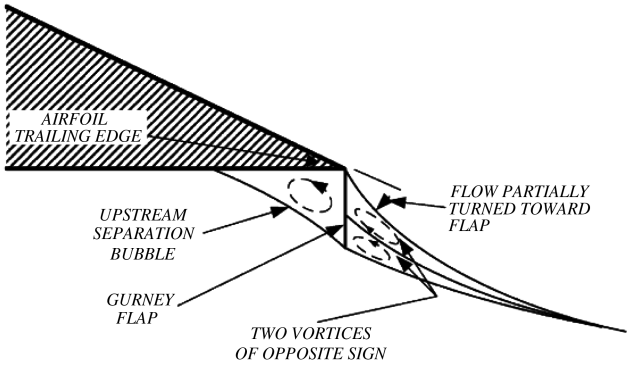


b)

**Fig. 2 The flow structure near the trailing edge (Liebeck [1]): a) conventional airfoil at moderate $C_L$ and b) hypothesized flow near a Gurney flap.**

corrupted by this device. An alternative is the jet Gurney flap, which has the same function as the conventional Gurney flap and can solve the drag-increase problem in cruise.

Traub et al. [17] carried out wind-tunnel investigation to examine the possibility of using a jet flap for hingeless control of a NACA 0015 airfoil. The slot was located 2% chord upstream from the trailing edge. Tests included jet momentum coefficient variation and comparison with a Gurney flap located at the same location. The data showed that the jet flap generates lift and moment coefficient increments, which is similar to a 0.75% chord Gurney flap for the jet blowing momentum coefficient $C_\mu \approx 0.01$. However, whereas the conventional Gurney flap showed a zero-lift drag coefficient penalty, this was not presented for the jet flap. Analysis showed that the power required by the jet flap airfoil for similar lift and moment increments was less than that required by the Gurney flap airfoil at low incidence; this trait reverses at higher incidence.

Trevelyan et al. [18] used the shear stress transport $\kappa$-$\omega$ turbulence model to investigate the effects of standard and pneumatic Gurney flaps on the NACA 4415 airfoil. The results also indicated that the lift coefficients at a 4 deg angle of attack matched for three different momentum coefficients ($C_\mu = 0.005$, 0.01, and 0.02) with three different Gurney flap heights ($0.006c$, $0.015c$, and $0.024c$). Different from the drag penalty introduced by standard Gurney flap, the drags for the three cases with pneumatic Gurney flaps are reduced compared with that of the clear airfoil. By decomposing the drag into two parts, one caused by the pressure difference between the upper and lower surfaces of the airfoil and the other caused by the Gurney flap, they found that the drag increment of the airfoil with Gurney flap is due to the pressure difference between the upstream and downstream sides of the flap. With the pneumatic Gurney flap, the drag of the airfoil was dramatically reduced compared with that of the airfoil with mechanical Gurney flap. This conclusion is also supported by Jeffrey et al.'s [5] experimental data, which measured the surface pressure along the Gurney flap itself.

Although the jet Gurney flap is more attractive because it overcomes the drag penalty of a conventional Gurney flap, it needs an air source and pneumatic pipe to generate an efficient blowing jet. This is too critical for engineering applications. In the present study, we will propose a new kind of Gurney flap to replace the jet Gurney flap. The plasma actuator produces a blowing jet without a pneumatic system. Investigations on aerodynamic flow control based on a plasma actuator are now in expansion because it is fully electronic with no moving parts, it has extremely fast response and very low mass, it needs low input power, and it is easy to simulate its effect in numerical flow solvers [19]. In particular, it is flexible, and so it can be formed to various shapes and located on air vehicles with relative ease. There are no other known actuators that have such flexibility [20].

The plasma actuator considered here is based on surface dielectric-barrier discharge (DBD). This new discharge method was realized by Roth et al. [21] and protected by a U.S. patent since 1995. This surface plasma has considerably influenced the research on airflow control, because its simplicity allowed many researchers in aerodynamics to work on this subject, without necessarily being a specialist in plasma physics [22]. The single DBD plasma actuator consists of two electrodes: one exposed to the air and the other covered by dielectric material. The typical asymmetric electrodes configuration of the single dielectric-barrier discharge (SDBD) is shown in Fig. 3. Velocity measurements indicate that the primary result of the averaged plasma-induced flow is the formation of a wall jet that imparts momentum to the fluid [19]. In the present study, a SDBD

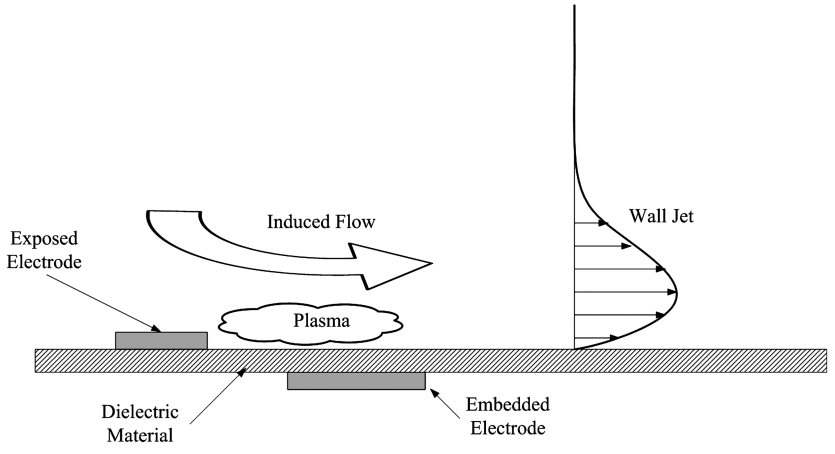


**Fig. 3 Sketch illustration of asymmetric electrodes SDBD plasma actuator and its induced wall-jet flow.**

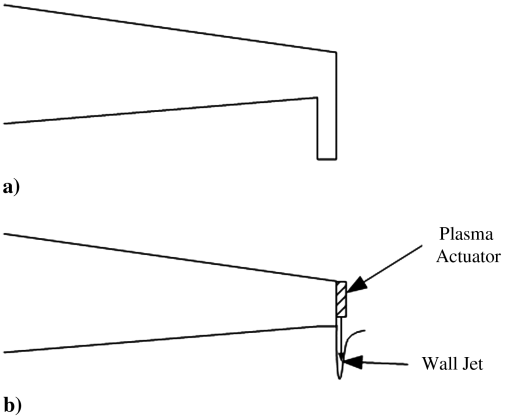


**Fig. 4 Sketches of the a) conventional Gurney flap and b) plasma Gurney flap**

plasma actuator indicated in Fig. 3 is attached to the aft surface of an airfoil (as shown in Fig. 4), and the plasma-induced wall jet will serve as a jet Gurney flap to alter the airfoil trailing-edge Kutta condition and to produce enough pressure difference between the upper and lower surfaces of the airfoil.

## Governing Equations and Numerical Method

In the present work, the plasma-induced body force is represented by a phenomenological model [23]. The method provides the primary control mechanism introduced by the plasma actuator, which, as described earlier, will yield a wall jet by momentum injection. Furthermore, recent computations [24], which compared the phenomenological model with a first-principle approach, demonstrate that the same qualitative flow control behavior is captured with both methodologies.

In this model, the flowfield is assumed to be described by the Reynolds-averaged Navier–Stokes (RANS) equations, augmented by terms representing the local forcing of the SDBD device [25]. For steady incompressible flow, the conservation of mass and momentum equations can be written as

$$\frac{\partial u_i}{\partial x_i} = 0 \qquad \rho\frac{\partial (u_i u_j)}{\partial x_j} + \frac{\partial p}{\partial x_i} = \frac{\partial \tau_{jj}}{\partial x_j} + F_i \tag{1}$$

In the momentum equation, the body force induced by the plasma actuator is given by

$$F_i = \vartheta \alpha \rho_c e_c \Delta t E_i \delta \tag{2}$$

where $\vartheta$ is the frequency of the applied voltage, $\alpha$ is a factor to account for the collision efficiency, $\rho_c$ is the electron number density, $e_c$ is the charge of the electron, $\Delta t$ (during which the plasma is formed) corresponds to one half-cycle, $E_i$ is the electric field strength in the $i$ direction, and $\delta$ is the Dirac delta function of space. The Dirac delta function means that the body force acts only in the regions in which the plasma is present [23]. The delta function ensures this restriction and is written as

$$\delta = \begin{cases} 1 & E > E_{\text{cr}} \\ 0 & E \le E_{\text{cr}} \end{cases} \tag{3}$$

All the computations presented here were carried out using the segregated solver in the FLUENT code. A steady form of RANS equations was used as the governing equations. The SIMPLE algorithm was used to generate steady-state solutions. The convection terms were discretized using the QUICK scheme, and the diffusion terms used second-order central differencing scheme. The high-order terms were treated using a deferred-correction approach. The discretized algebraic equations were solved using a pointwise Gauss–Seidel iterative algorithm. For this segregated solver, the convergence criteria used was to require the normalized residual to be less than $10^{-6}$ for the energy equation and less than $10^{-3}$ for all other equations.

The Spalart–Allmaras turbulence model [26] was selected as the turbulence model for all results discussed here. The Spalart–Allmaras model is robust and efficient and can handle general aerodynamic flows, including cases when flow separation and reattachment occur. In the model, the eddy viscosity is directly determined from the solution of a single transport equation. No ambiguous length scales need to be evaluated, as is the case with many previous algebraic and one-equation models. The model has been tested extensively. For high-lift flows, the Spalart–Allmaras model performs as well as higher-order models and better than algebraic and other one-equation models [27].

## Geometry Modeling and Grid Generation

In this study, the steady-state and two-dimensional computations were carried out on a NACA 0012 airfoil with a plasma Gurney flap. The chord length of the airfoil is 1 m, and the freestream velocity is 10 m/s. This yields a Reynolds number of $6.84 \times 10^5$, based on the airfoil chord length. The thickness of the airfoil trailing edge is 3 mm. A delta-shaped electric field induced by the plasma actuator is assumed to adhere to the trailing edge, with the height $a = 1.5$ mm and the width $b = 3$ mm. With the plasma actuator on, the ambient neutral air is absorbed by the plasma region and forms a wall jet, which is perpendicular to the lower surface of the airfoil trailing edge and serves as a jet Gurney flap (as show in Fig. 4b). The parameters adopted in the present study are the same as those in Shyy et al.'s [23] investigation, which used a typical SDBD plasma actuator configuration as in previous experimental study [28]. The various parameters here are the frequency of applied voltage $\vartheta = 3$ kHz, the charge-electron density $\rho_c = 1.03 \times 10^{11}/\text{cm}^3$, the applied voltage $U_a = 4$ kV rms, the breakdown electric field strength $E_b = 30$ kV/cm, the discharge time $\Delta t = 67$ $\mu$s, and the distance between the plates $d = 0.25$ mm. All of these parameters about the plasma actuator model have the same values as those in Roth et al.'s [28] experiment. Shyy et al. [23] also compared the induce velocity and the wall-jet velocity profile with the experiments, which match well with the real case, and so the plasma actuator model adopted in the present study is reasonable. More details about the electric field distribution and the body-force calculation can be seen in Shyy et al.'s paper.

To scale the strength of the plasma actuator, a nondimensional parameter $D_c$ is adopted to represent the ratio of the electrical force to the inertial force [25]. It is given by

$$D_c = \frac{q_c E_0 L}{\rho U_\infty^2} \tag{4}$$

where $q_c$ is the charge density and can be calculated as $\rho_c . e_c$; thus, the strength of plasma actuator $D_c$ in the present study is 9.14.

All of the computations were performed using a C-grid, as shown in Fig. 5a. The top and bottom far-field boundaries are 10 chord lengths from the airfoil. The upstream velocity inlet boundary is nine chord lengths away from the airfoil leading edge, and the downstream outflow boundary is 20 chord lengths away. The grid is constructed using the grid-generation code Gridgen. The algebraic stretching function of `TANH` is used to determine the circumferential and normal point distributions of the airfoil surface. To examine the effect of grid resolution on the aerodynamic forces, three structured 2-D grid systems (i.e., the coarse, medium, and fine cases) with grid points of $250 \times 75$, $350 \times 100$ and $450 \times 130$, respectively, are adopted. It is observed that the aerodynamic forces calculated with the medium grid and fine grid almost have no difference, but the forces with the coarse grid are a little smaller than those with the former two grid systems. Therefore, the medium grid is proper for the present study and is used in the following simulations.

Figure 5b shows a closer view of the grid in the vicinity of the airfoil trailing edge. The $1.5 \times 3.0$ mm plasma region adhered to the airfoil trailing edge is also included with a different shade. To add the body-force source term to the momentum equation in this region, the plasma region is defined as a separate control volume in FLUENT,

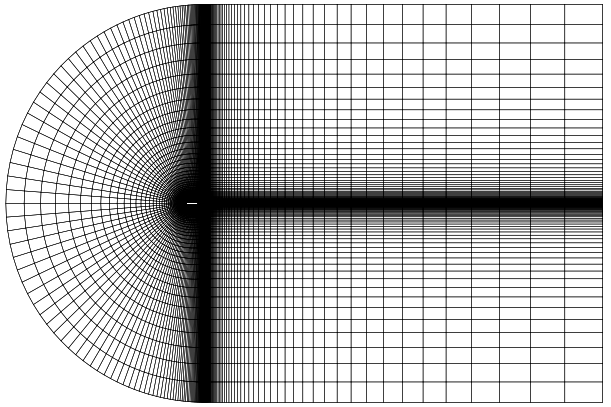

a)

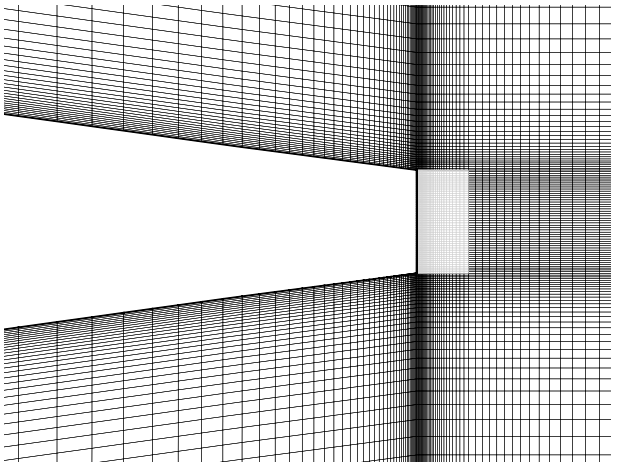

b)

**Fig. 5 C-grid system: a) the grid distribution around the airfoil and b) details of grid in the vicinity of the trailing edge, including the 1.5 × 3.0 mm plasma region.**

and the body force is added by user-defined function incorporated in FLUENT code. Grid clustering is evident near the surface of the airfoil, as well as near the trailing edge, to obtain reasonable resolution of the boundary layer and the plasma region. The first grid point above the surface is located at $y^+ \approx 1$.

## Results and Discussions

The validation of the numerical method used in the present study to simulate the plasma actuator induced flow has been done by Shyy et al. [23]. The predicted velocity profiles at different upstream and downstream locations match well with the experimental results. They also gave the effects of the incoming flow velocity, the applied voltage frequency, and the magnitude of the maximum wall-jet velocity induced by the plasma actuator. The results also had good agreement with theoretical analysis. In the present study, we just validate the accuracy of the numerical method to predict the aerodynamic characteristics of a NACA 0012 airfoil. The lift coefficient vs the angle of attack is plotted in Fig. 6, which contains the present simulated result and previous experimental data by different investigators [29–32]. Because the Reynolds numbers of these experiments vary from $1.6 \times 10^5$ to $3 \times 10^6$, the linear lift-curve slopes have a little difference and the stall angle of attack changes from 9 to 16 deg. The Reynolds number adopted in this paper is $6.84 \times 10^5$, and so the linear part of the lift curve falls in the divergence band of the experimental data, and the numerical predicted stall angle of attack is acceptable compared with the experimental data. Furthermore, the objective of the present study is to investigate the plasma Gurney flap on the aerodynamic modification of the airfoil before stall. In the linear region, the main

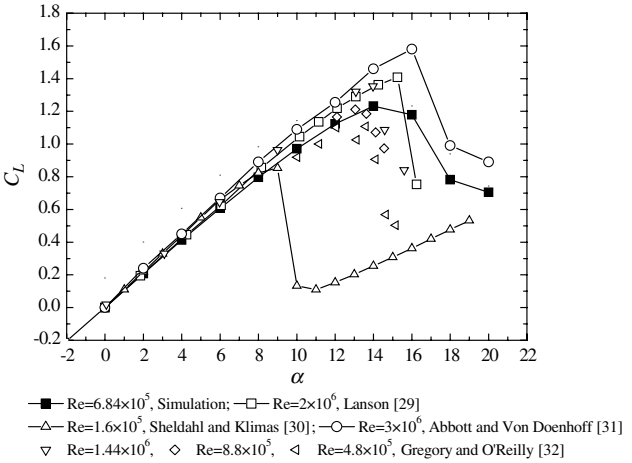


**Fig. 6 Lift coefficients of a NACA 0012 airfoil obtained in the present simulation and previous experimental studies.**

influence of the plasma Gurney flap is to alter the trailing-edge Kutta condition of the airfoil, which changes the airfoil camber. This effect can be regarded as the potential flow interaction without flow separation, and so the Spalart–Allmaras turbulence model is adequate for the present study. The comparison in Fig. 6 also supports this point.

Figure 7 presents the aerodynamic characteristics of the NACA 0012 airfoil with the plasma Gurney flap actuated on/off. It is obvious that the plasma Gurney flap at the trailing edge of the airfoil has much influence on the lift and pitching moment of the NACA 0012 airfoil. The linear part of the lift curve of the airfoil with the plasma Gurney flap is almost parallel with that of the clear airfoil, but with magnificent augmentation (in Fig. 7a). The zero-angle lift coefficient reaches 0.18. This feature is the same as that caused by a conventional Gurney flap on the NACA 0012 airfoil, both in experiments [33,34] and simulations [35]. The jet Gurney flap investigated in Traub et al.'s [17] experiment and Trevelyan et al.'s [18] numerical simulation presented the same effects on the lift and pitching moment of the NACA 0015 airfoil and NACA 4415 airfoil, respectively. These indicate that the plasma Gurney flap proposed in the present study has the same function as the conventional Gurney flap and the jet Gurney flap, and it can replace these two kinds of Gurney flap for its additional advantages, such as no moving parts, very fast-acting, more flexibility, etc. In the region after stall, the numerical results show that the effects of the plasma Gurney flap diminish. Because the flow over the upper surface of the airfoil is totally separated from the airfoil trailing edge and the plasma Gurney flap is immerged in the vortex wake, it cannot influence the flow around the airfoil, which is similar to the conventional Gurney flap. To improve the airfoil performance after stall, it is necessary to use an unsteady plasma Gurney flap, accounting for the airfoil's separated vortex-shedding frequency and the shear-layer instability frequency. This part needs further investigation in future work. Figures 7b and 7c present the lift vs drag (polar curve) and the lift-to-drag ratio vs the angle of attack, respectively. It is obvious that the drag coefficient of the NACA 0012 airfoil with the plasma Gurney flap is a little larger than that of the clean airfoil at the same lift coefficient before stall, but it is much less than the lift coefficient increment. This causes the lift-to-drag ratio to increase for the same angle of attack from 0 to 10 deg. Meanwhile, the maximum lift-to-drag ratio also increases. These features indicate that the plasma Gurney flap could avoid drag increase for the mechanical Gurney flap, which has been presented in previous experimental [33,34] and numerical [35] studies. With the lift enhancement, the quarter-chord nose-down pitching moment coefficient of the airfoil is increased, as shown in Fig. 7b. The pitching moment coefficient increment is one order less than the lift increment, but it is enough to provide moment for the aircraft's longitudinal flight control. By switching the plasma actuator on/off and changing the strength of the plasma-induced wall jet, the plasma Gurney flap can be considered as a hingeless control method for the

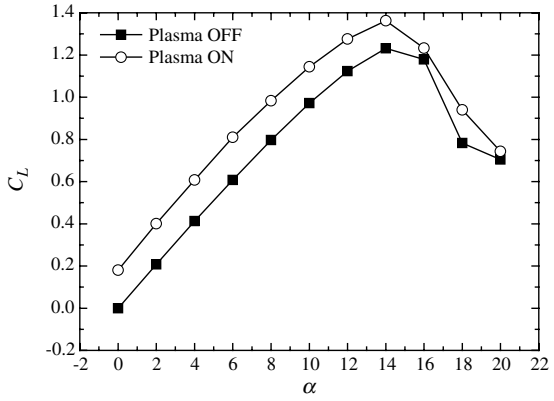


**a) Lift coefficient**

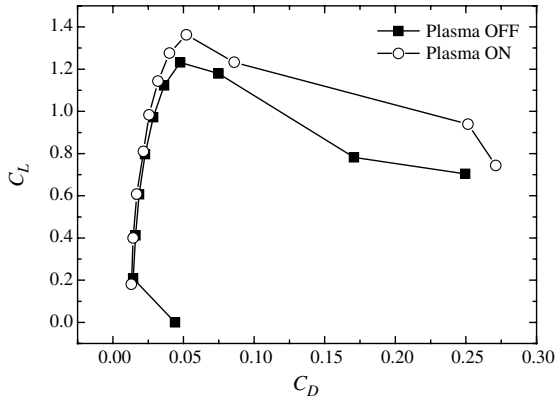


**b) Lift coefficient vs drag coefficient**

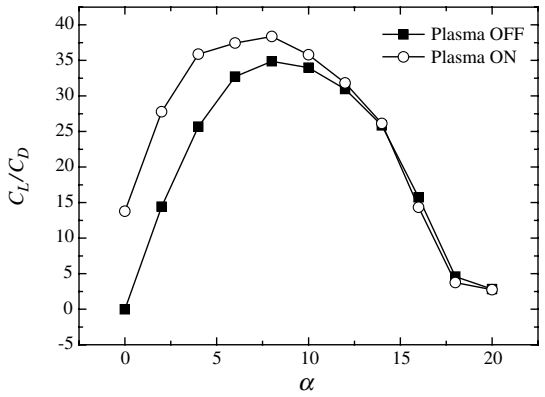


**c) Lift-to-drag ratio variation**

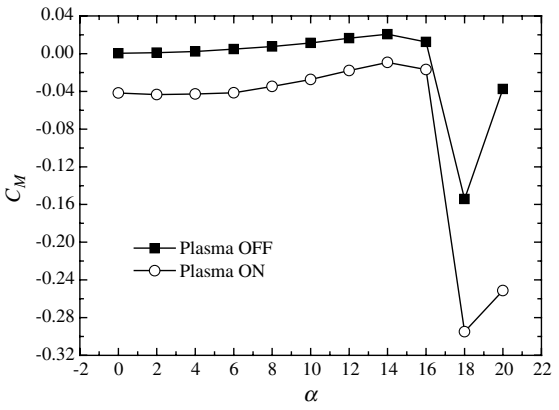


**d) Nose-down pitching moment**

**Fig. 7 Lift and pitching moment curve variations with/without a plasma Gurney flap.**

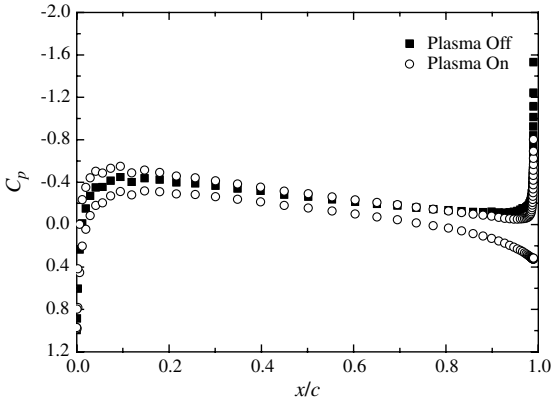


**a) $\alpha$=0 deg**

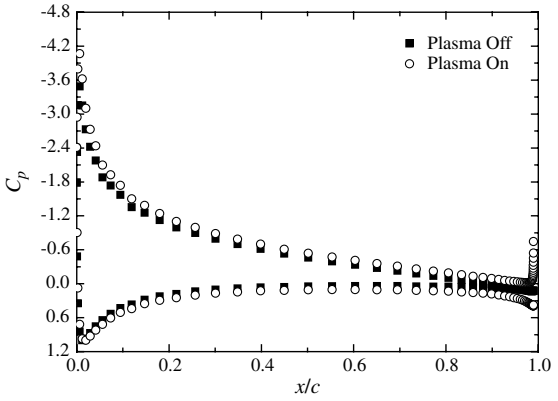


**b) $\alpha$=8 deg**

**Fig. 8 Pressure coefficient on the airfoil with/without a plasma Gurney flap.**

new concept aircraft, as indicated by Traub et al. [17] on the jet Gurney flap. Meanwhile, if the plasma Gurney flaps on the left and right wings of the aircraft are actuated asymmetrically, the roll and yaw movements can also be controlled by this active flow control method.

In addition to the integrated force and moment variation induced by the plasma Gurney flap, the changes of pressure coefficient around the airfoil with/without a plasma Gurney flap at $\alpha = 0$ and 8 deg are plotted in Fig. 8. The flap increases the pressure difference between the upper and lower surfaces, particularly in the vicinity of the trailing edge. This leads to the increased lift and additional nose-down pitching moment. The increase in trailing-edge loading was also observed in the experimental pressure distributions [5,33,34] and the numerical simulation results [4,18], which illustrates that the effect of the plasma Gurney flap on the increase manner of the airfoil loading is the same as that of the conventional Gurney flap.

To investigate the mechanism of a plasma Gurney flap on the airfoil, Fig. 9 gives the streamlines in the vicinity of the airfoil trailing edge and the contours of velocity magnitude. For a clean airfoil with 0.3% chord thickness at the trailing edge, the wake exhibits a shedding vortex similar to the wake of the bluff body (in Fig. 9a). With the plasma Gurney flap, the plasma actuator adhered to the aft surface of the airfoil produces a wall jet with a maximum velocity of about 10 m/s. The blowing jet is almost perpendicular to the trailing edge of the airfoil and serves as the Gurney flap. Although the direction of the plasma-induced jet deflects downstream, interacting with the flow from the lower surface of the airfoil, the jet can still block the flow on the lower surface near the airfoil trailing edge and produce a small separation bubble similar to that of a conventional Gurney flap [1] (as show in Fig. 2). This flow structure is the key for the plasma Gurney flap to enhance the lift of the airfoil. Another change of the flow structure is that the von Kármán vortex street disappears in the wake of the airfoil. For the jet Gurney flap, it can reduce the drag of airfoil compared with that of a conventional

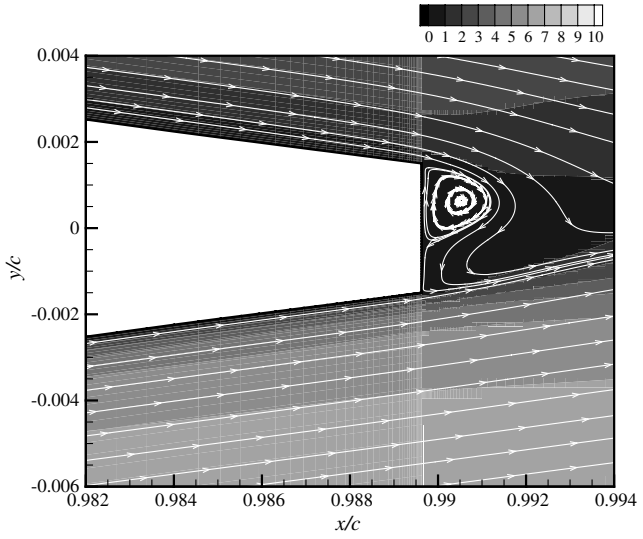


**a) Plasma off**

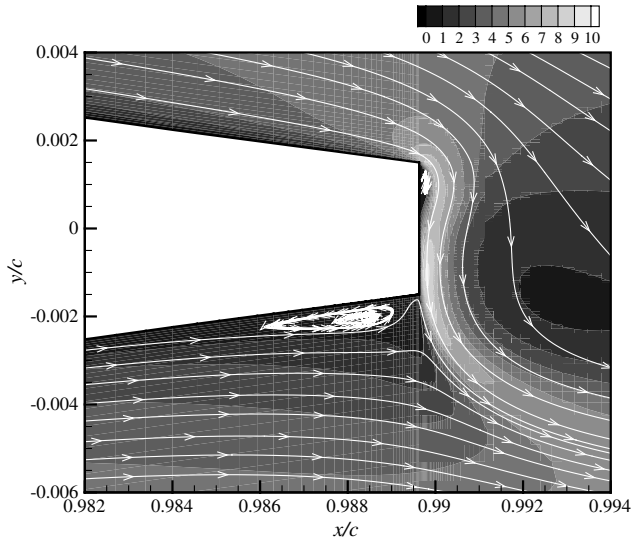


**b) Plasma on**

**Fig. 9 Details of the flowfield near the trailing edge of the NACA 0012 airfoil with the plasma Gurney flap switch on/off at $\alpha = 8$ deg.**

Gurney flap, because the main part of the drag comes from the pressure difference between the upstream and downstream sides of the Gurney flap, as indicated by Jeffrey et al. [5] and Trevelyan et al. [18]. But the jet slot usually locates about 2% chord upstream from the trailing edge to set the pneumatic system, and so the flow separated from the upper surface of the airfoil will interact with the flow from the lower surface and the von Kármán vortex street forms [18]. With advantage of flexibility and with no moving parts required, the plasma actuator can be adhered to the aft surface of the airfoil, and the flow from the upper surface of the airfoil will be absorbed into the plasma region, and so the flow separation is prevented and the von Kármán vortex street is eliminated. This characteristic of the plasma Gurney flap is favorable to the drag reduction compared with the jet Gurney flap, and so the lift-to-drag ratio of the NACA 0012 airfoil shown in Fig. 7c increases before stall.

The plasma Gurney flap is a circulation control device, similar to a jet flap, which increases the circulation of the airfoil by the flap-induced positive-camber effect and shifting the location of the Kutta condition. It is totally different from the circulation control device using the Coanda effect, as indicated by Trevelyan et al. [18]. For the Coanda circulation control airfoil, the essential condition is the rounded trailing edge, and so the jet can adhere to the airfoil surface and push the separation point aft to the lower surface of the airfoil. In the present case, the airfoil is cut at the trailing edge (as shown in Fig. 9), and so it has a flat-plate back surface with two sharp edges. The plasma-induced wall jet separated from the trailing edge serves as a jet flap, and so the separation point is fixed at the lower trailing edge and will not change with the strength of the jet, compared with that on a circulation control airfoil based on the Coanda effect. Because the trailing edge is sharp, the drawback for the plasma Gurney flap is the separation bubble on the aft surface of the airfoil near the upper trailing edge, which may cause a little drag increase. In the next step, the upper trailing edge could be rounded to suppress this flow separation bubble, and a new effect for jet flow control called the Coanda effect can be integrated with the plasma Gurney flap.

To scale the effect of the plasma Gurney flap on the aerodynamic modification of the airfoil, Fig. 10 compares the lift and quarter-chord pitching moment increments of the airfoil at zero angle of attack induced by present plasma Gurney flap and the conventional Gurney flap in previous experimental studies [33,34,36,37]. The experimental data in these papers have small divergence. The lift and pitching moment obtained by Li et al. [33] and Lee [36] have good agreement. The lift increment at zero angle of attack in the two experiments is higher than that of Jeffrey and Hurst [34], whereas the pitching moment is much smaller. Recently, Liu and Montefort [38] predicted the increments of lift coefficient and pitching moment coefficient of the airfoil induced by mechanical Gurney flap using thin-airfoil theoretical interpretation. They theoretically predicted that lift and pitching moment curves all matched well with the experimental data of Li et al. [33]. Furthermore, the ratio of the lift coefficient increment to the pitching moment coefficient increment is independent of the height of the Gurney flap by Liu and Montefort's analysis [38], which should be a constant as $\Delta C_L/\Delta C_M \approx -4$. The experimental data of Li et al. [33] support this, but the ratio from Jeffrey and Hurst's data [34] is about $-0.94$, which is far from the theoretically predicted value. We prefer to use the data of Li et al. [33] and Lee [36] for comparison, and the experimental data of the other two papers [34,37] are just plotted in the figure for reference. Because the objective of the present study is to coarsely estimate the effect of a plasma Gurney flap, the divergence of the experimental data will not affect the present conclusion. From the lift and pitching moment

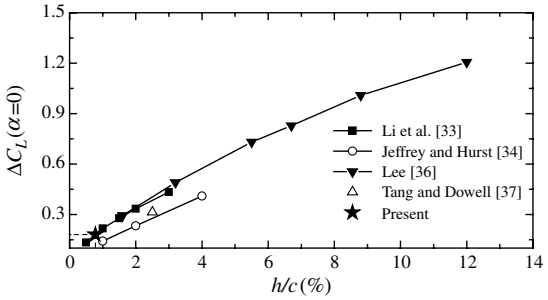


**a) Lift coefficient increment at zero angle of attack**

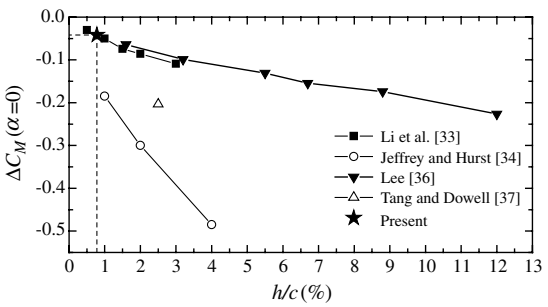


**b) Quarter-chord pitching moment increment at zero angle of attack**

**Fig. 10 Effect of plasma Gurney flap to increase the lift and nose-down pitching moment of the airfoil compared with that of the conventional Gurney flap.**

plots, the data all suggest that the plasma Gurney flap with $D_c = 9.14$ in the present study has the same effect as a 0.78% chord height conventional Gurney flap. From this estimation, it is convenient to extend the results in the conventional Gurney flap studies to the plasma Gurney flap. In the study of Traub et al. [17] about the jet Gurney flap, they concluded that the jet Gurney flap generates lift and moment coefficient increments similar to a 0.75% chord conventional Gurney flap for the jet blowing momentum coefficient $C_\mu \approx 0.01$. The plasma Gurney flap used in the present study is comparable with the jet Gurney flap with the jet blowing momentum coefficient $C_\mu \approx 0.01$.

## Conclusions

A novel type of Gurney flap, the plasma Gurney flap, is proposed in the present study. The plasma Gurney flap is a jet flap without pneumatic source by attaching the plasma actuator to the aft surface of the airfoil, which produces a wall jet perpendicular to the lower surface of the trailing edge of the airfoil and serves as the Gurney flap. The effect of the plasma Gurney flap on the aerodynamic characteristics of the NACA 0012 airfoil is studied by solving the two-dimensional steady incompressible Reynolds-averaged Navier–Stokes (RANS) equations. The plasma actuator is modeled by a adding body-force source term to the momentum equations.

The results indicates that the plasma Gurney flap can increase the lift and nose-down moment of the airfoil in the same way as the conventional Gurney flap. The main feature of the flow pattern and the loading variation on the airfoil are also similar to that of the conventional airfoil. Furthermore, with the plasma Gurney flap, the von Kármán vortex street downstream of the airfoil trailing edge, which is present in the wake of the conventional Gurney flap, disappears. This leads to the drag reduction of the NACA 0012 airfoil with Gurney flap and improves the lift-to-drag ratio performance of the airfoil.

By comparing the increment of the lift and nose-down pitching moment among the plasma Gurney flap, the conventional Gurney flap, and the jet Gurney flap, the results suggest that the plasma actuator used in present as the Gurney flap with the strength $D_c = 9.14$ has the comparable effect of a 0.78% chord height conventional Gurney flap and a jet Gurney flap with the jet blowing momentum coefficient $C_\mu \approx 0.01$.

## Acknowledgments

The present research was supported by the National Natural Science Foundation of China under grant no. 10872021 and the Aviation Creative Foundation of China under grant no. 07A51001.

## References

[1] Liebeck, R. H., "Design of Subsonic Airfoils for High Lift," *Journal of Aircraft*, Vol. 15, No. 9, 1978, pp. 547–561. doi:10.2514/3.58406

[2] Giguère, P., Dumas, G., and Lemay, J., "Gurney Flap Scaling for Optimum Lift-to-Drag Ratio," *AIAA Journal*, Vol. 35, No. 12, 1997, pp. 1888–1990. doi:10.2514/2.49

[3] Neuhart, D. H., and Pendergraft, O. C. Jr., "A Water Tunnel Study of Gurney Flaps," NASA TM 4071, 1988.

[4] Jang, C. S., Ross, J. C., and Cummings, R. M., "Computational Evaluation of an Airfoil with a Gurney Flap," AIAA Paper 92-2708, 1992.

[5] Jeffrey, D., Zhang, X., and Hurst, D. W., "Aerodynamics of Gurney Flaps on a Single Element High Lift Wing," *Journal of Aircraft*," Vol. 37, No. 2, 2000, pp. 295–301. doi:10.2514/2.2593

[6] Chandrasekhara, M. S., Martin, P. B., and Tung, C., "Compressible Dynamic Stall Performance of Variable Droop Leading Edge Airfoil with a Gurney Flap," AIAA Paper 2004-0041, 2004.

[7] Rhee, M., "A Computational Study of an Oscillating VR-12 Airfoil with a Gurney Flap," AIAA Paper 2004-5202, 2004.

[8] Bieniawski, S., and Kroo, I. M., "Flutter Suppression Using Micro-Trailing Edge Effectors," AIAA Paper 2003-1941, 2003.

[9] Lee, H., Kroo, I. M., and Bieniawski, S., "Flutter Suppression for High Aspect Ratio Flexible Wings Using Micro Flaps," AIAA Paper 2002-1717, 2002.

[10] Yen, D. T., van Dam, C. P., Bräeuchle, F., Smith, R. L., and Collins, S. D., "Active Load Control and Lift Enhancement Using MEMS Translational Tabs," AIAA Paper 2000-2422, 2000.

[11] Myose, R., Papadakis, M., and Heron, I., "Gurney Flap Experiments on Airfoils Wings, and Reflection Plane Model," *Journal of Aircraft*, Vol. 35, No. 2, 1998, pp. 206–211. doi:10.2514/2.2309

[12] Li, Y. C., Wang, J. J., Tan, G. K., and Zhang, P. F., "Effects of Gurney Flaps on the Lift Enhancement of a Cropped Nonslender Delta Wing," *Experiments in Fluids*, Vol. 32, No. 1, 2002, pp. 99–105. doi:10.1007/s003480200010

[13] Wang, J. J., Zhan, J. X., and Zhang, W., "Application of a Gurney Flap on a Simplified Forward-Swept Aircraft Model," *Journal of Aircraft*, Vol. 43, No. 5, 2006, pp. 1561–1564. doi:10.2514/1.20283

[14] Albertani, R., "Wind Tunnel Study of Gurney Flaps Applied to Micro Aerial Vehicle Wing," *AIAA Journal*, Vol. 46, No. 6, 2008, pp. 1560–1562. doi:10.2514/1.35110

[15] Wang, J. J., Li, Y. C., and Choi, K. S., "Gurney Flap—Lift Enhancement, Mechanisms and Applications," *Progress in Aerospace Sciences*, Vol. 44, No. 1, 2008, pp. 22–47. doi:10.1016/j.paerosci.2007.10.001

[16] Meyer, R., Hage, W., Bechert, D. W., Schatz, M., and Thiele, F., "Drag Reduction on Gurney Flaps by Three-Dimensional Modifications," *Journal of Aircraft*, Vol. 43, No. 1, 2006, pp. 132–140. doi:10.2514/1.14294

[17] Traub, L. W., Miller, A., and Rediniotis, O., "Comparisons of a Gurney and Jet-Flap for Hinge-Less Control," *Journal of Aircraft*, Vol. 41, No. 2, 2004, pp. 420–423. doi:10.2514/1.6023

[18] Trevelyan, C., Zahle, F., Michelsen, J. A., Søensen, N. N., and Infield, D. G., "A Computational Comparison of Standard and Pneumatic Gurney Flaps Using CFD. Scientific Proceedings," *European Wind Energy Conference and Exhibition*, European Wind Energy Association, Brussels, 22–25 Nov. 2004, pp. 112–116.

[19] Corke, T. C., Post, M. L., and Orlov, D. M., "SDBD Plasma Enhanced Aerodynamics: Concepts, Optimization and Applications," *Progress in Aerospace Sciences*, Vol. 43, Nos. 7–8, 2007, pp. 193–217. doi:10.1016/j.paerosci.2007.06.001

[20] Greenblatt, D., Kastantin, Y., Nayeri, C. N., and Paschereit, C. O., "Delta Wing Flow Control Using Dielectric Barrier Discharge Actuators," *AIAA Journal*, Vol. 46, No. 6, 2008, pp. 1554–1560. doi:10.2514/1.33808

[21] Roth, J. R., Tsai, P. P., Liu, C., Laroussi, M., and Spence, P. D., "One Atmosphere, Uniform Glow Discharge Plasma," U.S. Patent 5,414,324, issued 9 May 1995.

[22] Moreau, E., "Airflow Control by Nonthermal Plasma Actuators," *Journal of Physics D: Applied Physics*, Vol. 40, No. 3, 2007, pp. 605–636. doi:10.1088/0022-3727/40/3/S01

[23] Shyy, W., Jayaraman, B., and Andersson, A., "Modeling of Glow-Discharge Induced Fluid Dynamics," *Journal of Applied Physics*, Vol. 92, No. 11, 2002, pp. 6434–6443. doi:10.1063/1.1515103

[24] Gaitonde, D. V., Visbal, M. R., and Roy, S., "A Coupled Approach for Plasma-Based Flow Control Simulations of Wing Sections," AIAA Paper 2006-1205, 2006.

[25] Gaitonde, D. V., Visbal, M. R., and Roy, S., "Control of Flow Past a Wing Section with Plasma-Based Body Forces," AIAA Paper 2005-5302, 2005.

[26] Spalart, P. R., and Allmaras, S. R., "A One-Equation Turbulence Model for Aerodynamic Flows," AIAA Paper 92-0439, 1992.

[27] Rogers, S. W., Menter, F. R., Durbin, P. A., and Mansour, N. N., "A Comparison of Turbulence Models in Computing Multi-Element Airfoil Flows," AIAA Paper 94-0291, 1994.

[28] Roth, J. R., Sherman, D. M., and Wilkinson, S. P., "Electro Hydrodynamic Flow Control with a Glow Discharge Surface Plasma," *AIAA Journal*, Vol. 38, No. 7, 2000, pp. 1166–1172. doi:10.2514/2.1110

[29] Lanson, C. L., "Effects of Independent Variation of Mach and Reynolds Numbers on the Low-Speed Aerodynamic Characteristics of the NACA 0012 Airfoil Section," NASA Langley Research Center, TM-4074, Hampton, VA, 1988.

[30] Sheldahl, R. E., and Klimas, P. C., "Aerodynamic Characteristics of Seven Airfoil Sections Through 180 Deg Angle of Attack for Use in Aerodynamic Analysis of Vertical Axis Wind Turbines," Sandia

National Labs., Rept. SAND 80-2114, Albuquerque, NM, March 1981.
[31] Abbott, I. H., and Von Doenhoff, A. E., *Theory of Wing Sections*, Dover, New York, 1959, p. 462.
[32] Gregory, N., and O'Reilly, C. L., "Low Speed Aerodynamic Characteristics of a NACA 0012 Aerofoil Section, Including the Effects of Upper-Surface Roughness Simulating Hoar Frost," Aeronautical Research Council, Reports and Memoranda No. 3726, London, Jan. 1970.
[33] Li, Y. C., Wang, J. J., and Zhang, P. F. "Effect of Gurney Flaps on a NACA 0012 airfoil," *Flow, Turbulence and Combustion*, Vol. 68, No. 1, 2002, pp. 27–39.
doi:10.1023/A:1015679408150
[34] Jeffrey, D. R. M., and Hurst, D. W., "Aerodynamic of the Gurney Flap," AIAA Paper 96-2418, 1996.
[35] James, C. D., and Stephen, R. T., "Computational Evaluation of the Periodic Performance of a NACA 0012 Fitted with a Gurney Flap," *Journal of Fluids Engineering*, Vol. 124, 2002, pp. 227–234.
doi:10.1115/1.1427927
[36] Lee, T., "Aerodynamic Characteristics of Airfoil with Perforated Gurney-Type Flaps," *Journal of Aircraft*, Vol. 46, No. 2, 2009, pp. 542-548.
doi:10.2514/1.38474
[37] Tang, D., and Dowell, E. H., "Aerodynamic Loading for an Airfoil with an Oscillating Gurney Flap," *Journal of Aircraft*, Vol. 44, No. 4, 2007, pp. 1245–1257.
doi:10.2514/1.26440
[38] Liu, T. S., and Montefort J., "Thin-Airfoil Theoretical Interpretation for Gurney Flap Lift Enhancement," *Journal of Aircraft*, Vol. 44, No. 2, 2007, pp. 667–671.
doi:10.2514/1.27680

M. Glauser
*Associate Editor*